Scientia Iranica F (2023) 30(6), 2223–2234

SCIENTIA IRANICA

Sharif University of Technology

Scientia Iranica

Transactions F: Nanotechnology

http://scientiairanica.sharif.edu

Numerical treatment of magneto hydrodynamic Carreau liquid with heat and mass transport containing gyrotactic microorganisms

R. Naz, M. Sohail*, **M. Bibi, and M. Javed**

Department of Applied Mathematics and Statistics, Institute of Space Technology, Islamabad 44000, P.O. Box 2750, Pakistan.

Received 10 September 2019; received in revised form 18 April 2021; accepted 6 September 2021

KEYWORDS

Analytical solution;
Magneto-hydrodynamics (MHD);
Carreau nanofluid;
Gyrotactic microorganism;
Rotating disk;
Contour plot.

Abstract. In the current examination, insightful approximations are researched for magnetohydrodynamics Carreau nanofluid having gyrotactic microorganisms over a warmed turning plate. The plate is moving with the steady uniform rakish speed. Administering conditions are gotten by utilizing certain actual presumptions as incomplete differential conditions with limit conditions. These nonlinear types of conditions are changed into coupled standard differential conditions utilizing bunch likeness change. Optimal homotopy investigation strategy Optimal Homotopy Asymptotic Method (OHAM) is utilized to acquire the graphical outcomes and even qualities for the stream field factors. Graphical portrayal of speeds, temperature, fixation and thickness of gyrotactic microorganisms are examined and clarified. It is tracked down that dimensionless microorganism's fixation develops for bioconvective Lewis number and focus distinction variable of microorganisms. It is additionally seen that dimensionless speeds diminish because of the attractive impact and Carreau liquid boundary. Contour plots and mathematical outcomes are given for neighbourhood motion boundaries like skin rubbing coefficient, Nusselt number, Sherwood number and thickness number of motile microorganisms.

1. Introduction

Most of fluids in industry and common field like mud, sauce, printer ink, polymers, liquid cleaning agents, blood transport system, etc are significant non-Newtonian fluids typically. As non-Newtonian fluids conveys physical and mathematical association between shear rate and shear stresses. It is grouped into shear thickening, decreasing and dilatant fluids. In this manner number of constitutive explanation for such kind of fluid are proposed by specific examiners. Not at all like, power-law model which is customarily known as thickness subordinate Carreau fluid model. It is relevant for both low and high shear rates. This model is at first introduced through Carreau [1,2]. Khan et al. [3] considered the comportment of Carreau liquid model numerically by fluctuating and expanding sheet. Bilal et al. [4] thought warm detachment with alluring field. In that, converse Carreau liquid lead are seen for $n > 1$ and for $n < 1$ shear thickening and decreasing fluid separately and warm partition depicted warm dissemination of fluid stream. 3D effect of Carreau model by using impact of homogenous-heterogeneous reaction over broadened surface has been poor somewhere near

*. *Corresponding author.*
E-mail address: muhammad_sohail111@yahoo.com (M. Sohail)

doi: 10.24200/sci.2021.54398.3731

Irfan et al. [5]. Kefayati and Tang [6] analyzed basic convection stream of Magneto-hydrodynamics (MHD) Carreau fluid entropy age sway over warmed indirect chambers by using Boltzmann technique.

Nanofluids are used for achieving better warm conductivity in heat move measure. It has wide extent of different applications including space, shield, oils, ice chests, exhausting collaboration, water warming in close planetary framework and devices cooling, etc. The nanofluid stating is from the outset used by Choi and Eastman [7]. Khanafer and Vafai [8] mulled over the nanofluid application in various kinds of energy close by planetary gathering. Nanofluid are used by Munyalo and Zhang [9] to review the effect of atom size on some thermophysical properties. Sajid and Ali [10] are essentially researched on overhaul of warm conductivity of mutt nanofluids. Magneto-nanofluid over vertical broadened surface is considered by Rehman et al. [11].

Rotation are most helpful idea in numerous applications including PC gadgets, gas turbine, innovation of food handling, clinical hardware's thus numerous different applications through pivoting surfaces for example tube shaped turn, sheet revolution and plate pivot and so on Quite possibly the main space of examination is turning circle for non-Newtonian liquid. At first, turning plate wonders is utilized by Karman [12]. As of late, Hayat et al. [13] dissected entropy age impact over turning plate for Sisko liquid stream. The stream characteristics are reconnoitred by Lai et al. [14] from the skewed stream over turning and warmed plate. Hassan et al. [15] incited the assessment on the condition of iron nanoparticles by taking ferrofluid with rotating plate. The numerical results are gotten by Lok et al. [16] on rotational stagnation-point of axisymmetric stream under contracting/expanding rotational circle.

Motile gyrotactic microorganisms are those little living thing which are swim uninhibitedly with no external force. These natural substances are negligible thick than base fluid at first. They all around swim up way, which causing extension in base fluid thickness explicitly bearing. During this suspension, thickness point produces which is known as bioconvection. From the outset, the word bioconvection is used by Platt [17]. There is a touch contrast among nanofluid and gyrotactic microorganisms. Qayyum et al. [18] examined the radiation sway with gyrotactic microorganisms and nanofluid stream over a turning circle. The bioconvection pattern of nanoparticles with responsibility of gyrotactic microorganisms through mass progress convection are represented by Iqbal et al. [19]. Likewise, direct of magneto Maxwell nanofluid depiction with gyrotactic microorganisms is bankrupt somewhere around Khan et al. [20]. Thermoelectric impact and microorganisms are utilized by Sivaraj et al. [21].

Right now, Optimal Homotopy Asymptotic Method (OHAM) is used by Marinca et al. [22] which is applied for bothering techniques that is free for assumptions of little limits for the plan of nonlinear issues. OHAM was applied in different applications in different kind of fluids which are explored in [23–30]. Hosseinzadeh et al. [31] studied the inclusion of hybrid nanoparticles with different shape factors in water based micropolar fluid. They considered the involvement of natural convection by studying the thermal transport. Hosseinzadeh et al. [32] examined the bioconvection flow phenomenon in cross fluid over a stretching cylinder. They used an effective numerical package to obtain the solution of modelled Cross fluid transport problem. They plotted the comportment of numerous involved parameters on the solution profiles. Rostami et al. [33] examined the hydro thermal analysis in a porous enclosure by considering the comportment of ethylene glycol nanoparticle. They plotted the streamlines and contour plot to describe the behaviour of transport phenomenon against numerous emerging parameters. Das et al. [34] studied the phenomenon of thermal transport on couple stress magneto radiated model past over an exponential stretching sheet. The flow is assumed to be flow in Darcy Forchheimer medium with ohmic heating. Comprehensive study has been made by Vinoth Kanna et al. [35] on fuels. Gholinia et al. [36] studied the behaviour of different base fluids suspended in CNTs. Utilization of silicon dioxide on heat transport is explored by Hosseinzadeh et al. [37]. Selimefendigil and Öztop [38] studied the involvement of mixed convection and magnetic field in porous enclosure numerically. Some important explorations covering the transport phenomenon are detailed in [39–45,46].

The main objective of this article is to scrutinize the flow of MHD [47–51] Carreau nanofluid with gyrotactic microorganisms [52] over rotating heated disk. Von-Karman [52] transformations are applied to transfigure partial differential equations to ordinary differential equations. In our next project, we will extend this work to power law model with slip effects and variable thermos physical properties. Also, the use of Cattaneo-Christov theory will be made. OHAM is used to plot the results graphically. The organization of the article is as follows:

- Introduction is given in section one;
- Mathematical formulation is developed in section two;
- Numerical solutions and analysis is given in sections three and four respectively;
- Concluding remarks are given in section five;
- At the end references are listed.

2. Mathematical formulation for the considered flow with transport phenomenon

This analysis emphasizes on the MHD flow of two dimensional incompressible Carreau nanofluid with motile gyrotactic microorganisms induced by rotating disk. The strength of magnetic field B_0 for boundary layer is acted along $z-$ direction (see Figure 1). Bio-convective pattern occurs due to movement of motile microorganisms from higher area of microorganisms to low region. Constitutive relationship of Carreau fluid model [1–5,10,52] is:

$$\tau^* = \left[\eta_0\left(1+\lambda^2\dot{\gamma}^2\right)^{\frac{n-1}{2}}\right]\dot{\gamma},$$

$$\dot{\gamma} = \sqrt{\frac{1}{2}\sum_i\sum_j \gamma_{ij}\gamma_{ji}},$$

where (n) the power index. This model has the following characteristics depending upon the power index:

- Reduces to Newtonian model for $n = 0$;
- Shear thinning nature for $0 < n < 1$;
- Pseudo-plastic or and when $n > 1$.

The microorganisms flux [51,52] is expressed as:

$$J - nV - n\hat{V} + D_m \nabla n = 0, \qquad \hat{V} = \left(\frac{bW_c}{\Delta C}\right)\nabla C.$$

After applying the boundary layer approximations, the above equations and the corresponding boundary conditions are expressed as follows which has been made with the following assumptions:

- MHD effect,
- Carreau fluid model,
- Rotating disc,

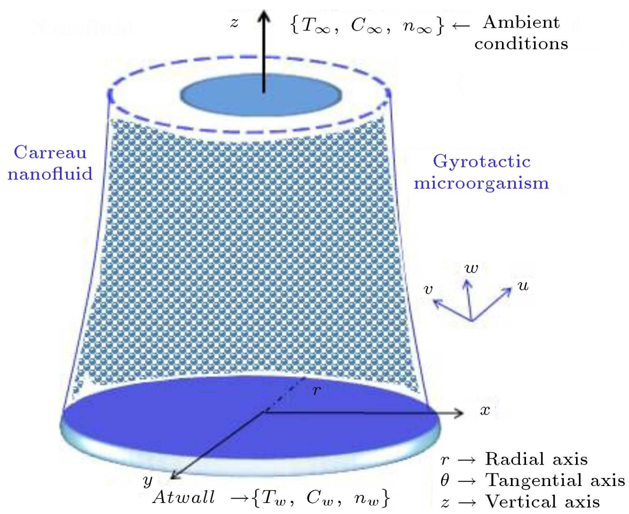

Figure 1. Physical model of flow configuration.

- No slip theory,
- Boungrino model,
- Mass transfer,
- Heat transfer,
- Conduction,
- Gyrotactic microorganisms.

$$\frac{\partial u}{\partial r} + \frac{u}{r} + \frac{\partial w}{\partial z} = 0, \tag{1}$$

$$\begin{aligned}
&\rho_f\left(u\frac{\partial u}{\partial r} - \frac{v^2}{r} + w\frac{\partial u}{\partial z}\right) - \frac{\partial^2 u}{\partial z^2}\eta_0 \\
&\quad - \frac{(n-1)}{2}\lambda^2\left\{\left(\frac{\partial v}{\partial z}\right)^2 + \left(\frac{\partial u}{\partial z}\right)^2\right\} \\
&\quad - 2\left(\frac{\partial v}{\partial z}\frac{\partial u}{\partial z}\right)^2 + \sigma B_0^2 u - \frac{(n-1)\,(n-3)}{8}\lambda^4 \\
&\quad \left\{\left(\frac{\partial v}{\partial z}\right)^4 + \left(\frac{\partial u}{\partial z}\right)^4 + 2\left(\frac{\partial v}{\partial z}\frac{\partial u}{\partial z}\right)^2\right\} \\
&\quad - \eta_0\frac{\partial u}{\partial z}\frac{\partial}{\partial z}\frac{(n-1)}{2}\lambda^2\left\{\left(\frac{\partial v}{\partial z}\right)^2 + \left(\frac{\partial u}{\partial z}\right)^2\right\} \\
&\quad - \frac{(n-1)\,(n-3)}{8}\lambda^4\left(\frac{\partial v}{\partial z}\right)^4 + \left(\frac{\partial u}{\partial z}\right)^4 = 0,
\end{aligned} \tag{2}$$

$$\begin{aligned}
&\rho_f\left(u\frac{\partial v}{\partial r} - \frac{u.v}{r} + w\frac{\partial v}{\partial z}\right) - \frac{\partial^2 v}{\partial z^2}\eta_0 \\
&\quad \left[1 + \frac{(n-1)}{2}\lambda^2\left\{\left(\frac{\partial v}{\partial z}\right)^2 + \left(\frac{\partial u}{\partial z}\right)^2\right\}\right. \\
&\quad + \sigma B_0^2 v - \frac{(n-1)\,(n-3)}{8}\lambda^4 \\
&\quad \left.\left\{\left(\frac{\partial v}{\partial z}\right)^4 + \left(\frac{\partial u}{\partial z}\right)^4 + 2\left(\frac{\partial v}{\partial z}\frac{\partial u}{\partial z}\right)^2\right\}\right] - \eta_0\frac{\partial v}{\partial z}\frac{\partial}{\partial z} \\
&\quad \left[\begin{array}{c} \frac{(n-1)}{2}\lambda^2\left\{\left(\frac{\partial v}{\partial z}\right)^2 + \left(\frac{\partial u}{\partial z}\right)^2\right\} \\ +\frac{(n-1)\,(n-3)}{8}\lambda^4 \\ \left\{\left(\frac{\partial v}{\partial z}\right)^4 + \left(\frac{\partial u}{\partial z}\right)^4 + 2\left(\frac{\partial v}{\partial z}\frac{\partial u}{\partial z}\right)^2\right\} \end{array}\right] = 0,
\end{aligned} \tag{3}$$

$$\begin{aligned}
&u\frac{\partial T}{\partial r} + w\frac{\partial T}{\partial z} - \alpha^*\frac{\partial^2 T}{\partial z^2} \\
&\quad - \tau\left[D_b\left(\frac{\partial T}{\partial z}\frac{\partial C}{\partial z}\right) + \frac{D_t}{T_\infty}\left(\frac{\partial T}{\partial z}\right)^2\right] = 0,
\end{aligned} \tag{4}$$

$$u\frac{\partial C}{\partial r}+w\frac{\partial C}{\partial z}-D_b\left(\frac{\partial^2 C}{\partial z^2}\right)-\frac{D_t}{T_\infty}\left(\frac{\partial^2 T}{\partial z^2}\right)=0, \quad (5)$$

$$u\frac{\partial n}{\partial r}+w\frac{\partial n}{\partial z}-D_m\left(\frac{\partial^2 n}{\partial z^2}\right)+\frac{bW_c}{\Delta C}\left(\frac{\partial}{\partial z}\left(n\frac{\partial C}{\partial z}\right)\right)=0, \quad (6)$$

$$u(r,z)=u_s\ (r)=l_0 r,\quad v(r,z)\ =r\Omega,\ w=0,$$

$$T=T_0,\ n=n_0,\ C=C_0,$$

$$\text{at}\quad z=0,\ u\to 0,\ v\to 0,\ T\to T_\infty,$$

$$n\to n_\infty,\ C\to C_\infty,\ \text{at}\quad z\to\infty. \quad (7)$$

3. Similarity variables

Considering the following transformations:

$$u-(r\Omega)\ f(\eta)=0,\quad v-(r\Omega)\ g(\eta)=0,$$

$$w-\left(\sqrt{\nu_f\Omega}\right)H(\eta)=0,\quad \eta=\left(\sqrt{\frac{\Omega}{\nu_f}}\right)z,$$

$$\theta(\eta)=\frac{T-T_0}{T_0-T_\infty},\quad \phi(\eta)=\frac{C-C_0}{C_0-C_\infty},$$

$$\xi(\eta)=\frac{n-n_\infty}{n_0-n_\infty}. \quad (8)$$

Dimensionless coupled system of ordinary differential equations is as follows:

$$H'-2f=0, \quad (9)$$

$$H'''-HH''-\tfrac{1}{2}(H')^2-\tfrac{g^2}{2}+\tfrac{n-1}{2}\lambda_1 Re\left[-H'''(g')^2-\tfrac{3}{4}(H'')^2H'''-H''g'g''\right]+\tfrac{(n-1)(n-3)}{8}(\lambda_1 Re)^2[-H'''(g')^4-\tfrac{5}{16}(H'')^4H'''-\tfrac{3}{2}(H'')^2(g')^2H'''-2H''g''(g')^3-(H'')^3g'g'']+MH'=0, \quad (10)$$

$$g''-Hg'-H'g+\tfrac{n-1}{2}\lambda_1 Re\left[\tfrac{1}{4}g''(H'')^2+3(g')^2g''+\tfrac{1}{2}H''g'H'''\right]+\tfrac{(n-1)(n-3)}{8}(\lambda_1 Re)^2 5g''(g')^4+\tfrac{1}{16}g''(H'')^4+\tfrac{3}{2}(H'')^2(g')^2g''+\tfrac{1}{4}g'H^{(iv)}(H'')^3+\tfrac{1}{4}(g')^3H''H''']-Mg=0, \quad (11)$$

$$\theta''+N_b\theta'\phi'+N_t(\theta')^2-PrH\theta'=0, \quad (12)$$

$$\phi''+\frac{N_t}{N_b}\theta''-Le\phi'=0, \quad (13)$$

$$\xi''-L_b\xi'H+Pe\left[\phi''(\xi-\Omega)+\xi'\phi'\right]=0, \quad (14)$$

$$\text{At}\quad \eta=0,\quad H=0,\quad H'=-2$$

s.t.:

$$g=1,\quad \theta=1,\quad \phi=1,\quad \xi=1,\quad \text{At}\quad \eta\to\infty,$$

$$H'=0,\quad g=0,\quad \theta=0,\quad \phi=0,\quad \xi=0. \quad (15)$$

3.1. Skin friction coefficient and local flux parameters

Formulation for local skin friction coefficients (C_f), Nusselt number (Nu), Sherwood number (Sh) and density of motíle microorganisms (Nn) are expressed as:

$$C_f=\frac{\sqrt{\tau_{rz}+\tau_{r\theta}}}{\rho_f(r\Omega)^2},\qquad Nu=\frac{rq_1}{k(T_0-T_\infty)},$$

$$Sh=\frac{rq_2}{D_b(C_\infty-C_0)},\quad Nn_r=\frac{rq_3}{Dm\,(n_\infty-n_0)}, \quad (16)$$

$$\tau_{rz}|_{z=0}=\frac{\partial u}{\partial z}\eta_0\left[1+\tfrac{(n-1)}{2}\lambda^2\left\{\left(\tfrac{\partial v}{\partial z}\right)^2+\left(\tfrac{\partial u}{\partial z}\right)^2\right\}+\tfrac{(n-1)(n-3)}{8}\lambda^4\left\{\left(\tfrac{\partial v}{\partial z}\right)^4+\left(\tfrac{\partial u}{\partial z}\right)^4+2\left(\tfrac{\partial v}{\partial z}\tfrac{\partial u}{\partial z}\right)^2\right\}\right] \quad (17)$$

$$\tau_{\theta z}|_{z=0}=\frac{\partial v}{\partial z}\eta_0\left[1+\tfrac{(n-1)}{2}\lambda^2\left\{\left(\tfrac{\partial v}{\partial z}\right)^2+\left(\tfrac{\partial u}{\partial z}\right)^2\right\}+\tfrac{(n-1)(n-3)}{8}\lambda^4\left\{\left(\tfrac{\partial v}{\partial z}\right)^4+\left(\tfrac{\partial u}{\partial z}\right)^4+2\left(\tfrac{\partial v}{\partial z}\tfrac{\partial u}{\partial z}\right)^2\right\}\right]$$

$$q_1=\left|-k\frac{\partial T}{\partial z}\right|_{z=0},\qquad q_2=\left|-D_b\frac{\partial C}{\partial z}\right|_{z-0},$$

$$q_3=\left|-D_m\frac{\partial n}{\partial z}\right|_{z=0}. \quad (18)$$

The expressions for dimensionless stress, heat transfer rate, mass transportation rate and the density number of microorganism profiles are:

$$C_fRe^{\frac{1}{2}}=\sqrt{(g')^2+(f')^2}\left[1+\lambda_1 Re\left((g')^2+(f')^2\right)\right]^{\frac{n-1}{2}},$$

$$NuRe^{-\frac{1}{2}}=-\theta'(0),\quad ShRe^{-\frac{1}{2}}=-\phi'(0),$$

$$Nn_rRe^{-\frac{1}{2}}=-\xi'(0). \quad (19)$$

4. Solution analysis and physical description

In the previous section, modelled equations have been approximated via OHAM. The proposed method is effective for the nonlinear problems and it has several important features. i.e.:

- It is free from discretization;
- No issue of domain for this scheme;
- No issue of nonlinearity;
- Free from small or large parameters assumption or requirement.

The upcoming discusses the comportment of different emerging parameters on solutions profiles. For this task several figures and tables are prepared to observe the comportment.

Figure 2 is plotted to perceive how the force record and Hartman number changes the speed. It is seen that for the expanding upsides of force law list, the speed decelerates because of expansion in the nonlinearity of given surface that upgrade resistive power. On escalating the Hartman number (M), physically, the Lorentz force will increase that in a result becomes more resistance between the flowing fluid particles. Consequently, fluid slows down for both shear thinning and thickening cases. As a result, velocity reduces due to the slow movement of fluid. The velocity field is read for Carreau liquid boundary and Hartman number in Figure 3. It is seen that the speed diminishes, for expansion in both the boundaries. It is also observed that an increment in λ_1 is indicates that the magnitude of velocity $f(\eta)$ decreases. Figure 4 is demonstrated that speed diminishes for the shear thickening liquid and furthermore for Hartman number. As Power-list differs, it acts as the shear thickening liquid thus shear diminishing layer would be little. Because of shear thickening conduct, speed profile will diminish. Similarly, it is shown that for the case of magnetic parameter (M), velocity of particles decays due to its resistive force, in which particles motion slows down.

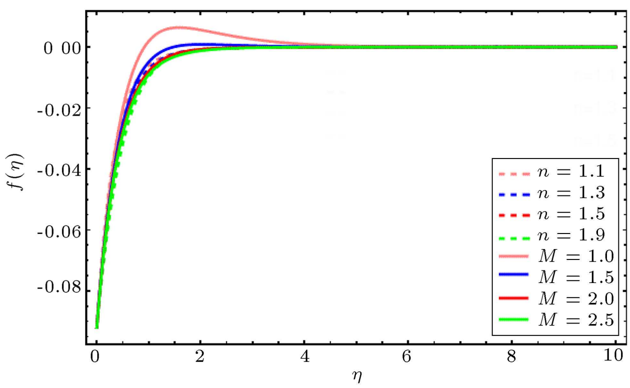

Figure 2. Comparison of n and M for $f(\eta)$.

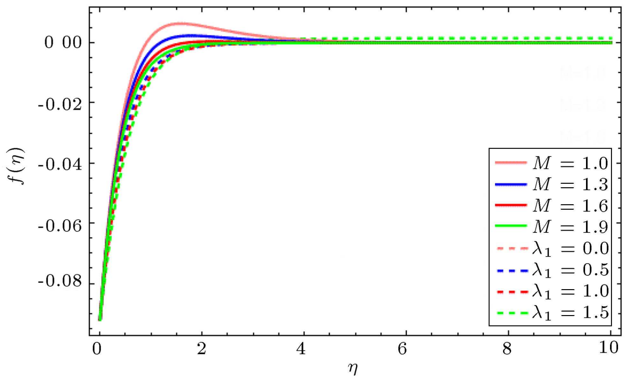

Figure 3. Comparison of M and λ_1 for $f(\eta)$.

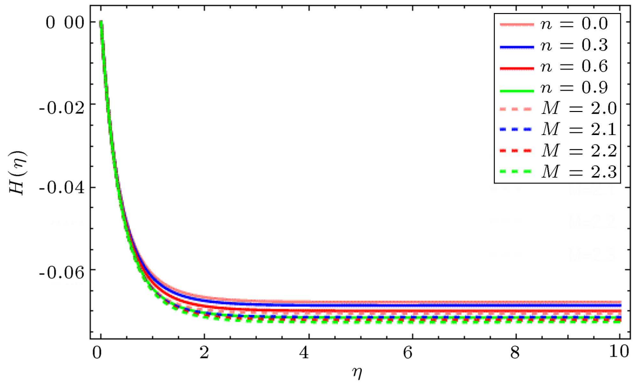

Figure 4. Comparison of n and M for $H(\eta)$.

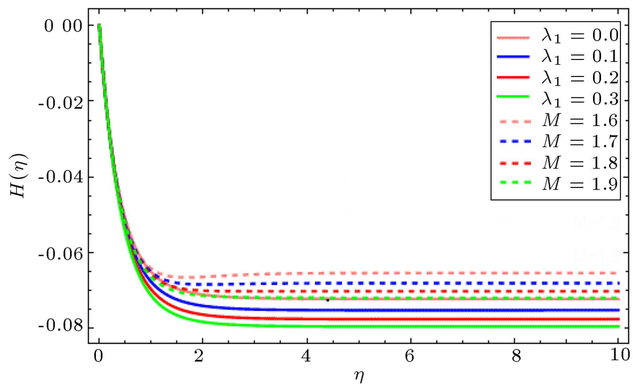

Figure 5. Comparison of λ_1 and M for $H(\eta)$.

Influence of the fluid parameter and the magnetic parameter on velocity profile is analyzed with the help of Figure 5. The comparable diminishing conduct is noticed for both the boundaries power-law and Hartman number on speed profile. The expanding power-law list and the Hartman number, shows the contrary impact on the speed profile which is explained through Figure 6. In this figure, the shear diminishing case, the stream speed of liquid particles upgrades for the worth of force list law. It is additionally seen that for enormous pace of attractive impact, frictional resistive power is expanded which go against the liquid molecule movement to help the velocity profile. In Figure 7, it

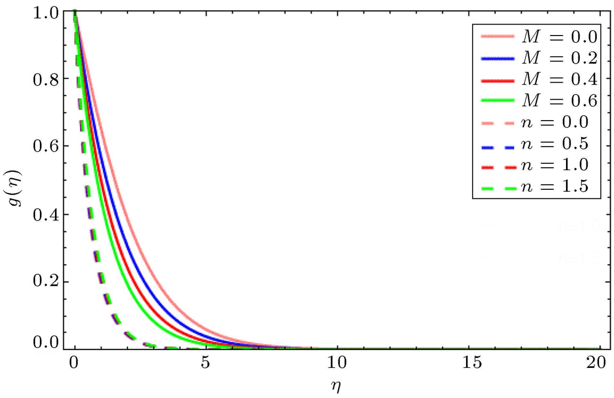

Figure 6. Comparison of M and n for $g(\eta)$.

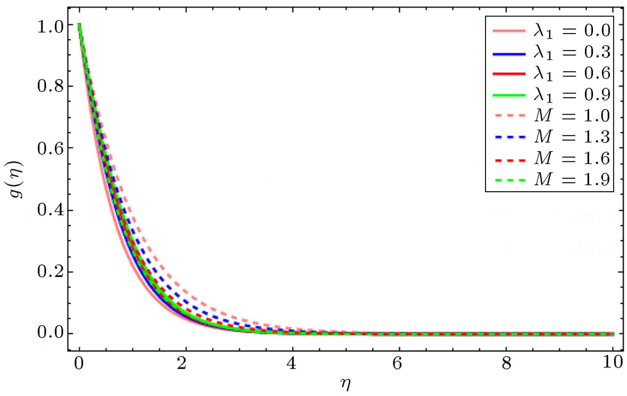

Figure 7. Comparison of λ_1 and M for $g(\eta)$.

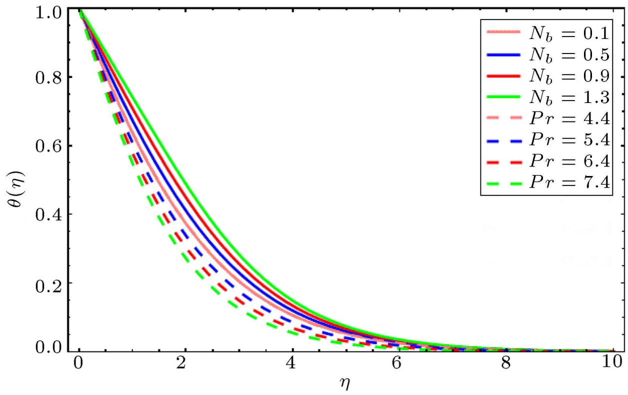

Figure 8. Comparison of N_b and Pr for $\theta(\eta)$.

is investigated that for an expanding worth of Carreau liquid boundary, the speed profile increments and as expanding worth of attractive boundary speed of liquid declines because of the Lorentz power. Improving the worth of Brownian movement boundary and Prandtl number, the temperature profile result acts in an unexpected way. It is uncovered in Figure 8, and it is seen that temperature profile increments because of the augmentation of Brownian movement boundary and shows decay by differing Prandtl number. Likewise saw that an addition in Prandtl number, warm layer thickness are diminishes, thusly, the temperature decreases.

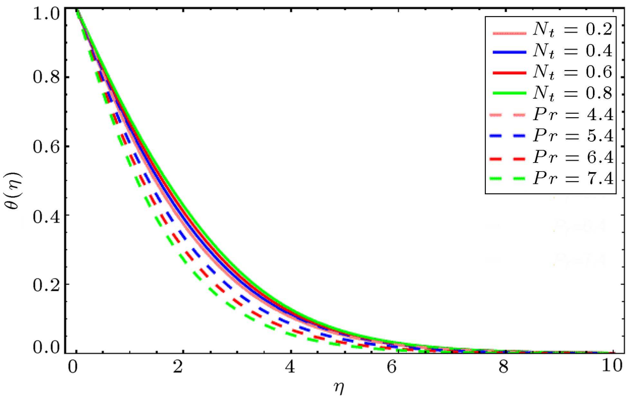

Figure 9. Comparison of N_t and Pr for $\theta(\eta)$.

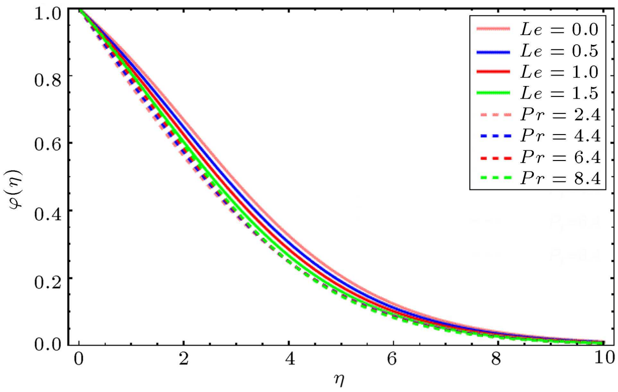

Figure 10. Comparison of Le and Pr for $\theta(\eta)$.

In thermophoresis measure, warmed liquid particles moves from hot to the virus surface. Therefore, liquid temperature improves. Both dimensionless boundaries act diversely for temperature profile. The effect of thermophoresis boundary and Prandtl number on temperature profile is appeared in Figure 9. Dimensionless Lewis boundary is the proportion of warm to mass diffusivity. By utilizing this, as diminishing in mass diffusivity, grouping of nanoparticles is declined. Since focus is identified with dissemination of mass developments. It gives the contrary outcome for fixation profile. As increase in momentum diffusivity concentration profile of nanoparticles $\varphi(\eta)$ is increased. Behavior of both parameters on $\varphi(\eta)$ is shown on Figure 10. Brownian movement boundary and Lewis number gives a similar effect on fixation profile which showed in Figure 11, higher Brownian movement boundary prompts higher arbitrary movement of liquid particles and lower mass development because of motor energy, in which fixation becomes rot. Additionally, for the enormous Lewis number, warm diffusivity expanded that prompts decrease in mass diffusivity. It is noticed that for higher upsides of bioconvective Lewis number, the diffusivity of swimming microorganisms in a turning plate reduced, along these lines the neighborhood grouping of microorganisms has been diminished. As an increase the Peclet number (Pe), the speed of swimming cells of

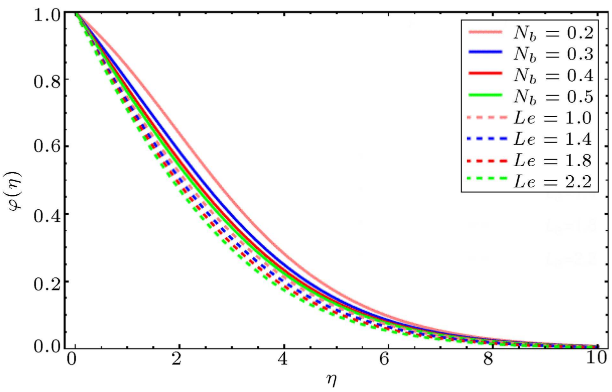

Figure 11. Comparison of N_b and Le for $\theta(\eta)$.

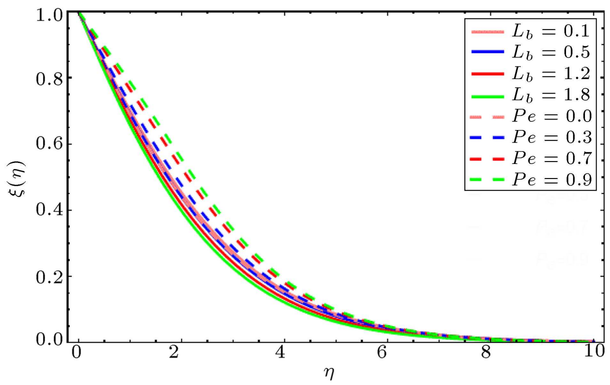

Figure 12. Comparison of L_b and Pe for $\xi(\eta)$.

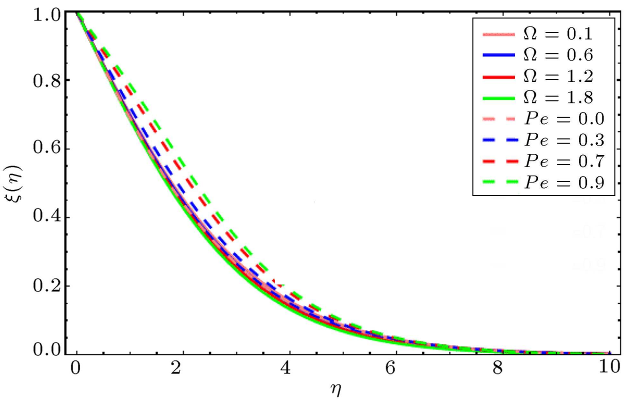

Figure 13. Comparison of Ω and Pe for $\xi(\eta)$.

microorganisms increased. Through this pattern concentration of motile microorganisms $\xi(\eta)$ in a moving disk will be increased. The graphical effect of these two boundaries on convergence of microorganisms is exhibited with the assistance of Figure 12. The impact of microorganisms focus contrast boundary and Peclet number on centralization of motile microorganisms is planned in Figure 13. For upgrading fixation distinction, builds the centralization of motile microorganisms for encompassing liquid yet shows decrease in the surface convergence of microorganism profile. Centralization of motile microorganisms has been upgrades as we expand the Peclet number.

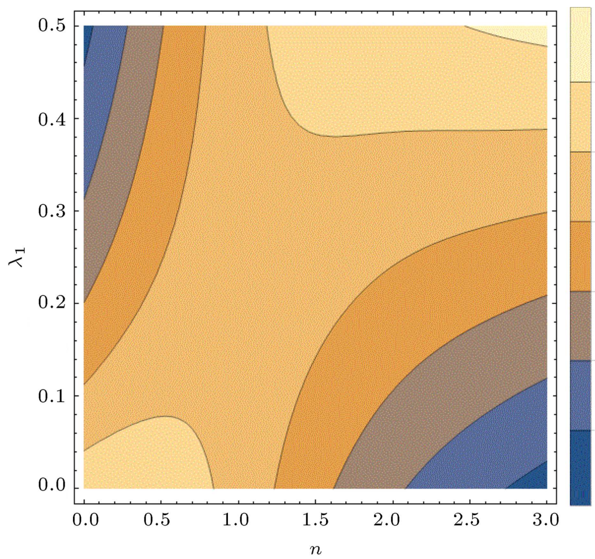

Figure 14. Plot of λ_1 and (n) for skin friction coefficient.

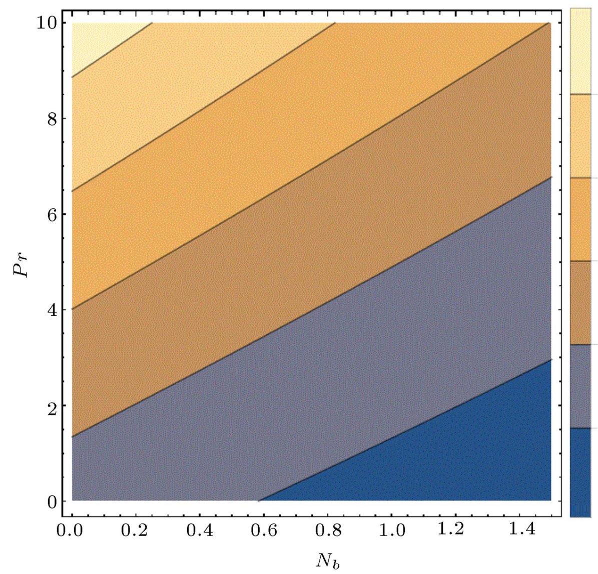

Figure 15. Plot of Pr and N_b for Nusselt number Nu_r.

5. Contour plots description

Figure 14 presents the contour plot for nearby grating coefficient for various upsides of force record law and Carreau liquid boundary. It shows inverse conduct for shear diminishing and thickening liquids. Shape plot for neighborhood Nusselt number and nearby Sherwood number with different upsides of dynamic boundaries Prandtl and Brownian movement boundary are portrayed in Figures 15 and 16 individually. For increasing N_b, conductive heat transfer occurs due to diffusion of nanoparticles that's decay the both numbers Nu and Sh. In case of Pr both shows the increasing behavior. Similarly contour plot for local density number of microorganisms Nn_r are plotted with active parameters Ω and Pe in Figure 17.

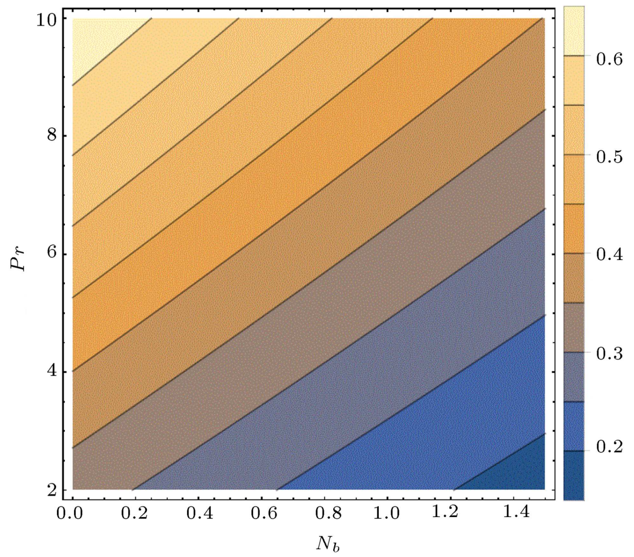

Figure 16. Plot of Pr and N_b for local Sherwood number.

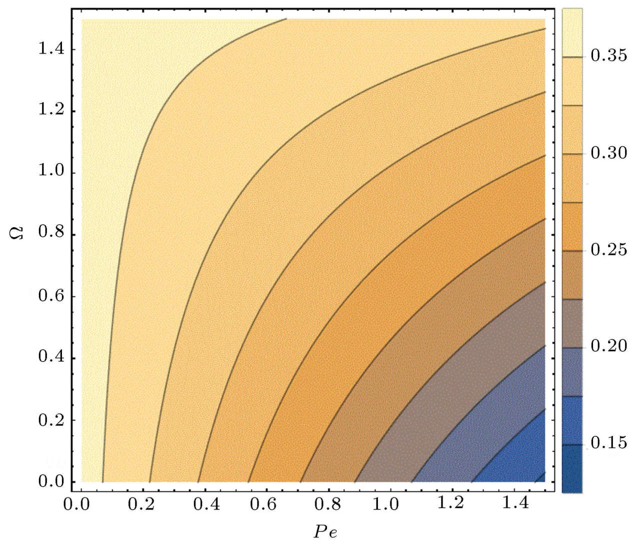

Figure 17. Plot of Ω and Pe for density of gyrotactic microorganisms.

6. Numerical solutions for different emerging parameters

Table 1 is prepared to notice the error analysis by OHAM by fixing the involved parameters. Table 2 presents the numerical results for dimensionless stress against magnetic parameter by fixing the other influential variables. It is recorded from the tabular results that magnetic parameter enhances the dimensionless stress. Physically, augmentation in magnetic parameter is responsible to retards the flow. It is observed that for large, the values of $C_f Re^{\frac{1}{2}}$ increases due to high friction resistance by fixing the other influential parameters. Table 3 discusses the augmentation of several parameters on heat transfer rate. Here, we aim to explore the comportment of Brownian motion parameter on (Nu). Tabulated data reveals the enhancement in (Nu) against (N_b). The magnitude of mass transportation rate is noted against different emerging parameters through Table 4. Escalation against Brownian motion parameter in mass transfer rate is recorded. Table 5 displayed the decreasing behavior of density of gyrotactic microorganisms for large values of Pe and L_b.

7. Finishing remarks and key outcomes of conveyed investigation

Transportation of warmth and mass for the progression of Carreau nanofluid with motile microorganisms has

Table 1. Error reduction against higher order approximations when $St = 0.39$, $M = 2.25$, $\lambda_1 = 0.9$, $Re = 1.2$, $Pr = 6.7$, $N_t = 0.1$, $N_b = 0.3$, $Le = 1.2$.

X	X_d^H	X_d^g	X_d^θ	X_d^φ	X_d^ξ	CPU time (s)
2	0.0002	0.0040	0.0020	0.0013	0.0270	0.29543
4	0.00007	0.0002	0.00030	0.00034	0.0053	2.40638
6	0.00002	0.00001	0.00002	0.00014	0.00039	10.9242
12	6.32×10^{-6}	7.92×10^{-6}	2.19×10^{-5}	0.000037	0.00004	58.9204
16	2.18×10^{-6}	1.62×10^{-6}	9.62×10^{-6}	7.74×10^{-5}	8.43×10^{-5}	64.4940
18	1.21×10^{-6}	8.75×10^{-7}	2.02×10^{-6}	9.85×10^{-6}	9.25×10^{-6}	78.8341
24	9.23×10^{-7}	4.63×10^{-7}	7.92×10^{-7}	6.47×10^{-6}	5.31×10^{-6}	98.9481
42	5.58×10^{-7}	9.84×10^{-8}	2.42×10^{-7}	8.73×10^{-7}	8.47×10^{-7}	308.842
50	2.48×10^{-8}	5.72×10^{-8}	8.13×10^{-8}	9.93×10^{-8}	5.29×10^{-7}	492.732
54	1.32×10^{-8}	2.73×10^{-8}	3.27×10^{-8}	4.83×10^{-8}	7.27×10^{-8}	537.847
60	6.72×10^{-9}	6.72×10^{-9}	1.63×10^{-8}	7.58×10^{-9}	4.21×10^{-8}	649.394
66	7.23×10^{-10}	4.21×10^{-10}	9.73×10^{-9}	5.74×10^{-9}	9.21×10^{-9}	843.639
70	3.76×10^{-10}	2.72×10^{-11}	5.57×10^{-10}	6.42×10^{-10}	2.36×10^{-9}	982.539

Table 2. Numerical results of skin friction coefficient $Re^{\frac{1}{2}}C_f(0)$ when $St = 0.09$, $M = 2.02$, $\lambda_1 = 0.9$, $Re = 1.2$, $Pr = 6.7$, $N_t = 0.1$, $N_b = 0.3$, $Le = 1.2$, $\Omega = 0.2$, $Pe = 0.7$, $L_b = 1.2$.

M	n	λ_1	Re	$Re^{\frac{1}{2}}C_f\ (0)$
0.1	1.0	0.5	0.9	0.423187
0.2	–	–	–	0.500069
0.3	–	–	–	0.572402
0.4	–	–	–	0.640583
0.1	2.0	0.5	0.9	0.429413
0.2	–	–	–	0.504486
0.3	–	–	–	0.576577
0.4	–	–	–	0.645889
1.0	1.0	0.5	0.9	0.981269
1.5	–	–	–	1.265467
2.0	–	–	–	1.490192
2.5	–	–	–	1.698251

Table 3. Computational results of $Re^{-\frac{1}{2}}Nu(0)$ when $St = 0.09$, $M = 2.02$, $n = 2.9$, $\lambda_1 = 0.9$, $Re = 1.2$, $\Omega = 0.2$, $Pe = 0.7$, $L_b = 1.2$.

N_b	N_t	Le	Pr	$Re^{-\frac{1}{2}}Nu\,(0)$
0.1	0.1	1.0	6.4	0.480056
0.2	–	–	–	0.463862
0.3	–	–	–	0.448108
0.4	–	–	–	0.432789
0.1	0.2	1.0	6.4	0.467692
0.2	–	–	–	0.451871
0.3	–	–	–	0.436486
0.4	–	–	–	0.421534

Table 4. Computation of local Sherwood number when $St = 0.29$, $M = 1.35$, $\lambda_1 = 0.2$, $Re = 1.4$, $\Omega = 0.5$, $Pe = 0.9$, $L_b = 1.5$.

N_b	N_t	Le	Pr	$Re^{-\frac{1}{2}}Nu\,(0)$
0.1	0.1	1.0	6.4	0.015659
0.2	–	–	–	−0.145346
0.3	–	–	–	−0.198832
0.4	–	–	–	−0.225441
0.1	0.2	1.0	6.4	−0.298010
0.2	–	–	–	−0.011591
0.3	–	–	–	−0.114436
0.4	–	–	–	−0.165596

been examined in current investigation. Optimal Homotopy Asymptotic Method (OHAM) is utilized to acquire the scientific arrangement of nonlinear coupled arrangement of changed standard differential conditions. The impact of different included variables on dimensionless speed, temperature, convergence of nanoparticles and centralization of motile microorganism's profiles are introduced graphically and afterward examined. The novel highlights of performed analysis are:

Table 5. Calculation for local density number when $St = 0.39$, $M = 2.25$, $\lambda_1 = 0.9$, $Re = 1.2$, $Pr = 6.7$, $N_t = 0.1$, $N_b = 0.3$, $Le = 1.2$.

Pe	L_b	Ω	$Re^{-\frac{1}{2}}Nn_r\,(0)$
0.1	0.5	0.2	0.324493
0.2	–	–	0.310349
0.3	–	–	0.296544
0.4	–	–	0.283021
0.1	1.0	0.2	0.340332
0.2	–	–	0.325989
0.3	–	–	0.311915
0.4	–	–	0.298117

- Power index shows inverse conduct on speed field on account of shear diminishing and shear thickening;
- Velocity field reduces against augmenting values of Hartman number and Carreau fluid parameter;
- Inverse comportment has been recorded on temperature field for Prandtl number and Brownian motion parameter;
- Temperature profile depreciate by enhancing Prandtl number;
- Augmentation in thermal profile is recorded against thermophoresis and Brownian motion parameters;
- Concentration lessens for Brownian motion parameter and it upsurges for Prandtl number;
- Convergence of motile microorganism's rots for bioconvective Lewis number and focus distinction variable of microorganisms and upgrades for Peclet number;
- Dimensionless stress grows against Hartman number;
- Mass transfer rate upsurges against Brownian motion parameter; whereas; heat transport rate diminishes.

Nomenclature

B_0	Magnetic field strength
l_0	Rate constant
u, v, w	Velocity components
Ω	Angular velocity
C_0	Initial
α^*	Thermal diffusivity
T	Temperature

D_b, D_t	Brownian and thermophoretic diffusion coefficients
N_b	Brownian motion parameter
Pe	Bioconvection Peclet number
Pr	Prandtl number
Re	Local Reynold number
λ_1	Carreau fluid parameter
C_f	Skin friction coefficients
(Nn_r)	Density of motile microorganisms
f, H, g	Dimensionless velocity
n	Power law index
C	Concentration
$U_s(r) = l_0 r$	Stretching velocity
r, θ, z	Spatial coordianates
C_∞	Ambient concentration
η_0	Viscosity of microorganism and suspension of nanofluid
ρ_f	Density of nanofluid
P	Fluid pressure
N_t	Thermophoresis motion parameter
L_b	Bioconvection Lewis number
St	Dimensionless stretching rate
M	Hartman number
Le	Lewis number
Nu	Nusselt number
Sh	Sherwood number
θ	Dimensionless temperature
φ	Dimensionless concentration

References

1. Carreau, P.J. "Rheological equations from molecular network theories", *Transactions of the Society of Rheology*, **16**(1), pp. 99–127 (1972).
2. Carreau, P.J. "An analysis of the viscous behavior of polymer solutions", *Can. J. Chem. Eng.*, **57**, pp. 135–140 (1979).
3. Khan, M., Malik, M.Y., Salahuddin, T., et al. "Numerical modeling of Carreau fluid due to variable thicked surface", *Results in Physics*, **7**, pp. 2384–2390 (2017).
4. Bilal, S., Alshomrani, A.S., Malik, M.Y., et al. "Analysis of Carreau fluid in the presence of thermal stratification and magnetic field effect", *Results in Physics*, **10**, pp. 118–125 (2018).
5. Irfan, M., Khan, M., and Khan, W.A. "Interaction between chemical species and generalized Fourier's law on 3D flow of Carreau fluid with variable thermal conductivity and heat sink/source: a numerical approach", *Results in Physics*, **10**, pp. 107–117 (2018).
6. Kefayati, G.R. and Tang, H. "MHD thermosolutal natural convection and entropy generation of Carreau fluid in a heated enclosure with two inner circular cold cylinders, using LBM", *International Journal of Heat and Mass Transfer*, **126**, pp. 508–530 (2018).
7. Choi, S.U. and Eastman, J.A. "Enhancing thermal conductivity of fluids with nanoparticles (No. ANL/MSD/CP-84938; CONF-951135-29). Argonne National Lab., IL (United States) (1995).
8. Khanafer, K. and Vafai, K. "A review on the applications of nanofluids in solar energy field", *Renewable Energy*, **123**, pp. 398–406 (2018).
9. Munyalo, J.M. and Zhang, X. "Particle size effect on thermophysical properties of nanofluid and nanofluid based phase change materials: A review", *Journal of Molecular Liquids*, **265**, pp. 77–87 (2018).
10. Sajid, M.U. and Ali, H.M. "Thermal conductivity of hybrid nanofluids: A critical review", *International Journal of Heat and Mass Transfer*, **126**, pp. 211–234 (2018).
11. Rehman, K.U., Alshomrani, A.S., and Malik, M.Y. "Carreau fluid flow in a thermally stratified medium with heat generation/absorption effects", *Case Studies in Thermal Engineering*, **12**, pp. 16–25 (2018).
12. Von Kármán, T. "Uber laminare und turbulente Reibung", *Z. Angew. Math. Mech.*, **1**, pp. 233–252 (1921).
13. Hayat, T., Khan, M.I., Qayyum, S., et al. "Entropy generation for flow of Sisko fluid due to rotating disk", *Journal of Molecular Liquids*, **264**, pp. 375–385 (2018).
14. Lai, W.C., Yin, P., and Liu, Y.H. "Investigation of flow characteristics from an inclined jet on a heated rotating disk", *International Journal of Heat and Mass Transfer*, **127**, pp. 943–956 (2018).
15. Hassan, M., Fetecau, C., Majeed, A., et al. "Effects of iron nanoparticles' shape on convective flow of ferrofluid under highly oscillating magnetic field over stretchable rotating disk", *Journal of Magnetism and Magnetic Materials*, **465**, pp. 531–539 (2018).
16. Lok, Y.Y., Merkin, J.H., and Pop, I. "Axisymmetric rotational stagnation-point flow impinging on a permeable stretching/shrinking rotating disk", *European Journal of Mechanics-B/Fluids*, **72**, pp. 275–292 (2018).
17. Platt, J.R. "Bioconvection patterns in cultures of free-swimming organisms", *Science*, **133**(3466), pp. 1766–1767 (1961).
18. Qayyum, S., Imtiaz, M., Alsaedi, A., et al. "Analysis of radiation in a suspension of nanoparticles and gyrotactic microorganism for rotating disk of variable thickness", *Chinese Journal of Physics*, **56**(5), pp. 2404–2423 (2018).
19. Iqbal, Z., Mehmood, Z., and Maraj, E.N. "Oblique transport of gyrotactic microorganisms and bioconvection nanoparticles with convective mass flux", *Physica E: Low-dimensional Systems and Nanostructures*, **88**, pp. 265–271 (2017).
20. Khan, M.I., Waqas, M., Hayat, T., et al. "Behavior of stratification phenomenon in flow of Maxwell nanomaterial with motile gyrotactic microorganisms in the

presence of magnetic field", *International Journal of Mechanical Sciences*, **131**, pp. 426–434 (2017).

21. Sivaraj, R., Animasaun, I.L., Olabiyi, A.S., et al. "Gyrotactic microorganisms and thermoelectric effects on the dynamics of 29 nm CuO-water nanofluid over an upper horizontal surface of paraboloid of revolution", *Multidiscipline Modeling in Materials and Structures*, **14**(4), pp. 695–721 (2018).

22. Marinca, V., Herişanu, N., and Nemeş, I. "Optimal homotopy asymptotic method with application to thin film flow", *Open Physics*, **6**(3), pp. 648–653 (2008).

23. Sohail, M. and Naz, R. "Modified heat and mass transmission models in the magnetohydrodynamic flow of Sutterby nanofluid in stretching cylinder", *Physica A: Statistical Mechanics and Its Applications*, **549**, 124088 (2020).

24. Sohail, M., Naz, R., and Bilal, S. "Thermal performance of an MHD radiative Oldroyd-B nanofluid by utilizing generalized models for heat and mass fluxes in the presence of bioconvective gyrotactic microorganisms and variable thermal conductivity", *Heat Transfer-Asian Research*, **48**(7), pp. 2659–2675 (2019).

25. Naz, R., Tariq, S., Sohail, M., et al. "Investigation of entropy generation in stratified MHD Carreau nanofluid with gyrotactic microorganisms under Von Neumann similarity transformations", *The European Physical Journal Plus*, **135**(2), 178 (2020).

26. Danish, M., Kumar, S., and Kumar, S. "A note on the solution of singular boundary value problems arising in engineering and applied sciences: Use of OHAM", *Computers and Chemical Engineering*, **36**, pp. 57–67 (2012).

27. Naz, R., Noor, M., Shah, Z., et al. "Entropy generation optimization in MHD pseudoplastic fluid comprising motile microorganisms with stratification effect", *Alexandria Engineering Journal*, **59**(1), pp. 485–496 (2020).

28. Sohail, M., Ali, U., Al-Mdallal, Q., et al. "Theoretical and numerical investigation of entropy for the variable thermophysical characteristics of couple stress material: Applications to optimization", *Alexandria Engineering Journal*, **59**(6), pp. 4365–4375 (2020).

29. Abdelsalam, S.I. and Sohail, M. "Numerical approach of variable thermophysical features of dissipated viscous nanofluid comprising gyrotactic microorganisms", *Pramana*, **94**(1), pp. 1–12 (2020).

30. Liao, S. "An optimal homotopy-analysis approach for strongly nonlinear differential equations", *Communications in Nonlinear Science and Numerical Simulation*, **15**(8), pp. 2003–2016 (2010).

31. Hosseinzadeh, K., Roghani, S., Asadi, A., et al. "Investigation of micropolar hybrid ferrofluid flow over a vertical plate by considering various base fluid and nanoparticle shape factor", *International Journal of Numerical Methods for Heat and Fluid Flow*, **31**(1), pp. 402–417 (2020).

32. Hosseinzadeh, K., Roghani, S., Mogharrebi, A.R., et al. "Investigation of cross-fluid flow containing motile gyrotactic microorganisms and nanoparticles over a three-dimensional cylinder", *Alexandria Engineering Journal*, **59**(5), pp. 3297–3307 (2020).

33. Rostami, A.K., Hosseinzadeh, K., and Ganji, D.D. "Hydrothermal analysis of ethylene glycol nanofluid in a porous enclosure with complex snowflake shaped inner wall", *Waves in Random and Complex Media*, pp. 1–18 (2020).

34. Das, S., Ali, A., and Jana, R.N. "Darcy-Forchheimer flow of a magneto-radiated couple stress fluid over an inclined exponentially stretching surface with Ohmic dissipation", *World Journal of Engineering*, **18**(2), pp. 345–360 (2020). https://doi.org/10.1108/WJE-07-2020-0258

35. Vinoth Kanna, I., Arulprakasajothi, M., and Eliyas, S. "A detailed study of IC engines and a novel discussion with comprehensive view of alternative fuels used in petrol and diesel engines", *International Journal of Ambient Energy*, **42**(115), pp. 1794–1802 (2019).

36. Gholinia, M., Hosseinzadeh, K., and Ganji, D.D. "Investigation of different base fluids suspend by CNTs hybrid nanoparticle over a vertical circular cylinder with sinusoidal radius", *Case Studies in Thermal Engineering*, **21**, 100666 (2020).

37. Hosseinzadeh, K., Ganji, D.D., and Ommi, F., "Effect of SiO_2 super-hydrophobic coating and self-rewetting fluid on two phase closed thermosyphon heat transfer characteristics: An experimental and numerical study", *Journal of Molecular Liquids*, **315**, 113748 (2020).

38. Selimefendigil, F. and Öztop, H.F. "Combined effects of double rotating cones and magnetic field on the mixed convection of nanofluid in a porous 3D U-bend", *International Communications in Heat and Mass Transfer*, **116**, 104703 (2020).

39. Selimefendigil, F. and Öztop, H.F. "Magnetohydrodynamics forced convection of nanofluid in multi-layered U-shaped vented cavity with a porous region considering wall corrugation effect", *International Communications in Heat and Mass Transfer*, **113**, 104551 (2020).

40. Naz, R., Mabood, F., Sohail, M. et al. "Thermal and species transportation of Eyring-Powell material over a rotating disk with swimming microorganisms: applications to metallurgy", *Journal of Materials Research and Technology*, **9**(3), May-June 2020, pp. 5577–5590 (2020).

41. Selimefendigil, F. and Öztop, H.F. "Mixed convection in a PCM filled cavity under the influence of a rotating cylinder", *Solar Energy*, **200**, pp. 61–75 (2020).

42. Khan, R.M., Ashraf, W., Sohail, M., et al. "On behavioral response of microstructural slip on the development of magnetohydrodynamic micropolar boundary layer flow", *Complexity*, **2020** (2020).

43. Selimefendigil, F. and Öztop, H.F. "MHD pulsating forced convection of nanofluid over parallel plates with blocks in a channel", *International Journal of Mechanical Sciences*, **157**, pp. 726–740 (2019).

44. Sohail, M., Nazir, U., Chu, Y.M., et al. "Computational exploration for radiative flow of Sutterby nanofluid with variable temperature-dependent thermal conductivity and diffusion coefficient", *Open Physics*, **18**(1), pp. 1073–1083 (2020).

45. Alsabery, A.I., Selimefendigil, F., Hashim, I., et al. "Fluid-structure interaction analysis of entropy generation and mixed convection inside a cavity with flexible right wall and heated rotating cylinder", *International Journal of Heat and Mass Transfer*, **140**, pp. 331–345 (2019).

46. Rashidi, M.M., Abelman, S., and Mehr, N.F. "Entropy generation in steady MHD flow due to a rotating porous disk in a nanofluid", *International journal of Heat and Mass transfer*, **62**, pp. 515–525 (2013).

47. Sheikholeslami, M., Rashidi, M.M., and Ganji, D.D. "Effect of non-uniform magnetic field on forced convection heat transfer of Fe_3O_4-water nanofluid", *Computer Methods in Applied Mechanics and Engineering*, **294**, pp. 299–312 (2015).

48. Rashidi, M.M., Ali, M., Freidoonimehr, N., et al. "Parametric analysis and optimization of entropy generation in unsteady MHD flow over a stretching rotating disk using artificial neural network and particle swarm optimization algorithm", *Energy*, **55**, pp. 497–510 (2013).

49. Rashidi, M.M., Kavyani, N., and Abelman, S. "Investigation of entropy generation in MHD and slip flow over a rotating porous disk with variable properties", *International Journal of Heat and Mass Transfer*, **70**, pp. 892–917 (2014).

50. Sheikholeslami, M., Vajravelu, K., and Rashidi, M.M. "Forced convection heat transfer in a semi annulus under the influence of a variable magnetic field", *International Journal of Heat and Mass Transfer*, **92**, pp. 339–348 (2016).

51. Alsaedi, A., Khan, M. I., Farooq, M., et al. "Magnetohydrodynamic (MHD) stratified bioconvective flow of nanofluid due to gyrotactic microorganisms", *Advanced Powder Technology*, **28**(1), pp. 288–298 (2017).

52. Bibi, M., Sohail, M., and Naz, R. "Theoretical analysis of MHD Carreau liquid over a heated rotating disk under Von-Karman transformations", *Multidiscipline Modeling in Materials and Structures*, **16**(2), pp. 390–408 (2019).

Biographies

Rahila NAZ is associated with the department of Applied Mathematics and Statistics, Institute of Space Technology (IST) Islamabad as an Associate Professor. Her area of research is about nanofluids, heat transfer, nonlinear science, MHD effects, blood flow and boundary value problems.

Muhammad Sohail belongs to a very small village of district Haripur, Khyber Pakhtunkhwa, Pakistan. He got his PhD mathematics degree from the Institute of Space Technology Islamabad, Pakistan in 2020. His research interests are on CFD simulation, mass transport, heat transfer, mathematical modelling, nonlinear dynamics, stability analysis, numerical and analytical methods, fractional differential equations, mixed convection and heat exchangers. He published about 56 research articles in different peer reviewed international journals.

Memoona Bibi completed her MSc mathematics degree from Institute of Space Technology Islamabad under the supervision of Dr. Naz. Her research interest includes bio-convection, non-Newtonian fluids, heat and mass transfer.

Maryam Javed is associated with the department of Applied Mathematics and Statistics, Institute of Space Technology (IST) Islamabad as an Associate Professor. Her area of research is about Hall effect, mass transfer, nanofluids, heat transfer, MHD effects, blood flow modelling, perturbation methods and partial differential equations.